Four-element division algorithm to focus coherent light through a turbid medium

Longjie Fang (方龙杰), **Cheng Zhang** (张 诚), **Haoyi Zuo** (左浩毅), **Jianhua Zhu** (朱建华), and **Lin Pang** (庞 霖)*

College of Physical Science and Technology, Sichuan University, Chengdu 610064, China
Corresponding author: panglin_p@yahoo.com

Aiming to overcome the low converging rate and susceptibility to the environment in focusing the coherent light through the turbid medium, four-element division algorithm (FEDA) optimization is proposed. Full levels of comparisons with the currently employed element-based algorithms, stepwise sequential algorithm (SSA), and continuous sequential algorithm (CSA) show that FEDA only takes one third of the measurement time to find the optimized solution, which means that FEDA is promising in practical applications, such as for deep tissue imaging.

OCIS codes: 290.0290, 260.3160.
doi: 10.3788/COL201715.102901.

Turbid media, such as wood, disordered metamaterials, and living tissues, are opaque because of the strong scattering of light[1–3]. For a long time, it is believed that light scattering is the fundamental limitation for light to propagate through turbid media. However, it was demonstrated that light could be focused to a sharp point after propagating through a strongly scattering turbid media by spatially shaping the wavefront of incident light[3]. The spatially shaped wavefront specifically depends on a certain configuration of the turbid medium. In other words, by controlling the incident wavefront to match the scattering effect of the turbid media, a sharp focus could be formed after propagating through turbid media[4].

Optical phase optimization approaches for fast focusing light through turbid media using an element-based phase control algorithm have been widely studied in recent years due to the rapid development of the spatial light modulator (SLM). The SLM is a phase modulated device on which the phase of each pixel can be controlled independently. Previously, the element-based algorithms, i.e., the stepwise sequential algorithm (SSA) and continuous sequential algorithm (CSA), were proposed[1,2]. For SSA, the optimal phase of an element is determined by cycling its phase from 0 to 2π, while the rest of the elements keep the optical phase the same as the incident beam. Upon the circulation, the phase with which the target intensity reaches highest is stored as the initial optimized phase for this element. After the optimization of all of the elements, the stored phases are employed on the corresponding elements, leading to the light focusing at the targeted position. In order to see the progress of the optimization processing, in other words, to see the intensity at the focal area increase, CSA was proposed. Instead of storing the pre-optimized phase for later use, the initially optimized phase is employed on the corresponding element following the circulation. Both SSA and CSA

involve optimization through one element after one element, called the single-element-based algorithm. The advantage of this approach is that the phase contribution of each element is very clear; however, because the intensity contribution of each element to the focal point is small, especially for the case of a large number of elements, the determination of the optimal phase for the single element would be difficult. In other words, the signal-to-noise ratio (SNR) of the measurement is weak, leading to a possibly local maximal during the optimization[3–10]. Moreover, the initial optimized phase pattern for each element after one iteration is the result of the constructive interference between the element and the background, or between the element and the previously optimized elements, not in phase with each other. Therefore, more iterations are needed to obtain the optimized phase distribution among all the elements[8–10].

On the other hand, the whole element optimization approaches, i.e., the partitioning algorithm (PA), transmission matrix (TM) approach, and genetic algorithm (GA), were introduced into the focusing in scattering media[2,7,11]. The PA maximizes the intensity of the target signal by modulating a randomly selected half of the elements during each measurement[2]. The TM approach is proposed to calculate the TM by monitoring the intensity in the output plane when the incident light is modulated[11–23]. The GA is a class of probabilistic optimization algorithms that are inspired by the biological evolution process and can be employed in focusing light through scattering media[7]. In these approaches, all elements are employed for the optimization, in which the SNR during the optimization is improved. However, because more random processings are introduced into the processing, optimizations take more time to converge than the single-element-based approach.

In this Letter, we propose the four-element division algorithm (FEDA) to accelerate the focusing procedure

and improve the signal-to-noise rate. Instead of optimizing the individual element in the processing, FEDA takes all of the elements into account during each optimization processing. The enhancement and converging rate of the focusing light through turbid media by using SSA, CSA, and FEDA are compared in detail by an experiment. By comparing the three approaches, it is concluded that the FEDA technique converges the processing faster than those of the SSA and CSA, since FEDA does not need any iteration. Moreover, the FEDA is less sensitive to noise environments due to the fact that a quarter of the total number of pixels changes simultaneously at the beginning, and the feedback signal is high.

First, we define some terminology employed in the context. A 'pixel' on the phase modulation plane is the smallest modulation unit that can be controlled separately in SLM. An 'element' on the SLM is a group of adjacent pixels of the phase modulation plane, which are combined and their phases change simultaneously. The format '$m \times n$' represents a phase plane with a horizontal number of elements of m and the vertical number of elements of n. An iteration refers to a whole processing to obtain the phase values of all the elements. For FEDA, all of the elements refer to the element number in the final layer. The general principle of element-based algorithms for focusing light is in the following paragraphs.

The incident wavefront is divided into N input modes and incident on a sample. The sample can be anything that mainly scatters light. Light propagating through the sample is completely diffused and has no correlation with the incident wavefront. Therefore, the intensity distribution in the receiving plane is the random speckle pattern, and the intensity at the targeted position, or focal point, is extremely weak. The element-based phase control algorithms optimize the incident wavefront by selecting the appropriate phase for each element to maximize the intensity at the focal point, which is called one measurement. The enhancement of the target signal is defined as the ratio between the optimized intensity and the intensity of the target area before optimization, which can be expressed as[3]

$$\eta = \frac{I_{\text{opt}}}{I_0}, \tag{1}$$

where η is the enhancement, I_{opt} is the target intensity after optimization, and I_0 is the initial intensity of the speckle pattern. During the optimization, the intensity of the focal point is defined by integrating the CDD value reading over the defined area of 10×10 pixels.

In SSA, the optimization takes place between the element and background, while in CSA the optimization is conducted by considering the contribution from the previously optimized elements and the background. Therefore, these two algorithms need to iterate at least two times. In order to avoid the iteration and further increase the SNR, we propose FEDA to make the optimization processing take the whole element into account. In FEDA, the total area of the phase modulation plane is initially divided equally into four elements. The optimization processing starts with cycling the optical phase of the first element from 0 to 2π, as shown in Fig. 1(a), while the target signal is monitored, and the phase value at which the target intensity gets the maximum is recorded and set into this element before the optimization takes place at the second elements, as is shown in Fig. 1(b). After the optimization, the second element is set to its optimized phase value; thus, the third element is optimized with the first, and the second element kept the optimized phase values [see Fig. 1(c)]. The fourth element is optimized with the rest of the three elements taking their optimized phase values, shown in Fig. 1(d), which lead to optimized 2×2 elements. Obviously, in FEDA, the contributions of all elements are considered. In other words, the optimization is obtained by interfering constructively from all of the elements, as is shown in Fig. 1(e). The optimized 2×2 format is called the first layer of the phase distribution plane.

Next, one element is further divided into four of the same elements, as is shown in Fig. 1(f). Each smaller element first inherits its first layer's phase distribution. Optimization takes place for each smaller element by cycling its phase from 0 to 2π, while the signal at the focal point is monitored, and the phase value at which the target intensity reaches the maximum is acquired and set to replace the inherited phase value from first layer before the optimization moves to the second smaller element, as shown in Fig. 1(g). The same processing is conducted to the rest of the smaller elements, shown in Figs. 1(h) and 1(i). The divisions and optimizations are employed to all four elements in the first layer. A 4×4 element phase array with all of its elements optimized is achieved, as shown in Fig. 1(j), which could be called the second layer of the phase distribution plane.
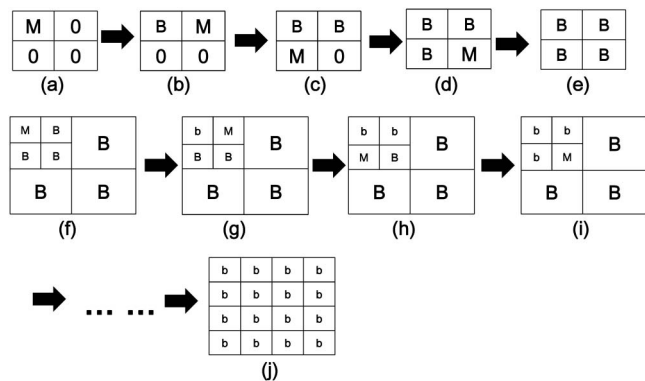

Fig. 1. Principle used in the FEDA to focus scattered light. (a)–(e) Procedure of phase modulation of four elements. (f)–(j) Procedure of phase modulation of 16 elements. M means to modulate these elements cycling from 0 to 2π; 0 represents the part that stays the same with the original wave; B is the element of the optimized phase of the elder generation; b is the element of the optimized phase of the filial generation.

The division and optimization could be continued to generate an 8×8 optimized phase array, the third layer of the phase distribution plane. This procedure can go on, generating 16×16, 32×32, ... optimized phase arrays, until the number of elements equals the number of pixels of the SLM.

The FEDA greatly improves the SNR of the measurement, since it starts with the large elements of phase modulation, in which the detector at the imaging plane easily catches the intensity variation when the phase modulation of $0–2\pi$ at the element takes place. Furthermore, as mentioned above, the optimization in FEDA happens on the layer-by-layer basis, in which optimization processing in the new generation layer always inherits the optimal phase distribution of the elder generation. In other words, FEDA itself is an 'iteration'-based optimization with the element size reduced at each iteration, leading to a high converging rate and high enhancement to focus through the turbid medium.

The focusing effect of the three algorithms is verified by focusing light through the turbid media experimentally. The turbid medium we use is a one sided ground glass. The total thickness of the ground glass is 4 mm. The illustration of the experimental setup is shown in Fig. 2. An He–Ne laser beam with a 632.8 nm wavelength is spatially filtered and collimated to become a plane wave after passing through a microscope objective O1 ($40\times$, NA = 0.65) and a lens L1 with a focal length of 100 mm. There is a pinhole at the back focal plane of microscopic objective lens O1. The diameter of the pinhole is 15 μm, and it can work as a spatial filter. The exit light from L1 is the plane wave, and it is incident on a phase-only SLM (Holoeye PLUTO-TELCO). The resolution of the SLM is 1920×1080 pixels, and the size of each pixel is 8 μm × 8 μm. The modulator is a twisted nematic liquid crystal device and can achieve phase-only modulation up to the 2π phase with 256 levels. The phase modulated light is reflected and redirected by a beam splitter (BS), then imaged on the surface of the ground glass by a demagnification system composed of lenses L2 (focal length of 300 mm) and L3 (focal length of 100 mm) and an objective lens ($10\times$, NA = 0.65). A $20\times$ objective lens (NA = 0.4) is used to image the rear surface of the ground glass onto a CCD camera (THORLABS). The resolution of the CCD is 2048×1152 pixels, and the size of each pixel is 6.75 μm × 6.75 μm. The images on the CCD camera are imported into a computer to calculate the intensity of the targeted area of 20×20 pixels (135 μm × 135 μm) as a feedback to optimize the incident phase by modulating the elements on the SLM.

Figure 3 shows the experimental enhancement in the three algorithms versus the measurements when element number $N = 4096$ (64×64) is employed. The step size of cycling the optical phase from 0 to 2π in the experiment is 0.2π. The SSA and CSA were performed for four iterations since they saturated after the fourth iteration. The dash lines in Fig. 3 indicate each iteration. It can be seen from Fig. 3(a) that for SSA the enhancement initially stays at the starting value, since a single element modulation of the SLM causes little influence on the signal detected at the CCD. When the measurement times reached 4096, or after an iteration of all of the elements, the target intensity increased abruptly since all the elements are set to their first optimized values, in which all elements interfere constructively at the defined focal point. After that, the second iteration starts since in the first iteration the optimization of each element was acquired by only taking into account of the contributions of the element itself, the background, and the interference between the element and the background. The interference among the elements was not considered. The second iteration is based on the previously optimized phase distribution. During the second iteration, the enhancement barely changed. After the second iteration, when each element was optimized again, the enhancement increases again. This process repeated four times in total; the enhancement values increased four times. The increased level of the enhancement after each iteration reduced dramatically; the enhancement almost saturates in the four iterations. From Fig. 3(b), it can be seen that for CSA the enhancement increases continuously during the optimization. The enhancement initially increases fast in the first iteration. The enhancement increases slowly in the second and third iteration and saturates in the fourth iteration, which means that the optimal phase distribution is very close to the ideal phase distribution. For FEDA, it can be seen
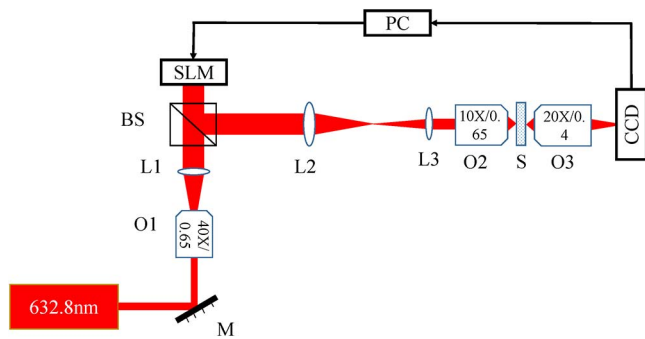

Fig. 2. Setup used to focus light through turbid media. M is a mirror; O1, O2, and O3 stand for microscope objectives; L1, L2, and L3 are lenses with a focal distance of 75, 300, and 100 mm, respectively; S represents the turbid medium or the ground glass; PC, personal computer.
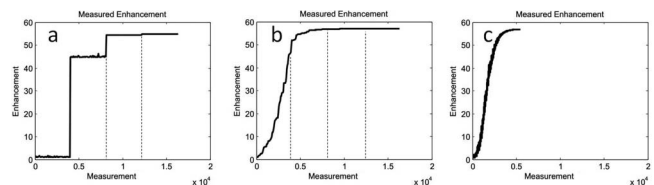

Fig. 3. Experimental enhancement of the three algorithms with respect to measurement times at the element number of 4096. (a) SSA with an iteration of four times, (b) CSA with an iteration four times, (c) FEDA.

from Fig. 3(c) that the enhancement increases continuously during the optimization with a much higher increase rate compared to SSA and CSA. FEDA reaches the optimization within 5460 measurements with almost the same enhancement value compared to CSA and SSA after 16,384 measurements.

For SSA and CSA, the optimizations were iterated four times, while in FEDA it was performed only once. The achieved enhancement is 56.7 and 58.5 for SSA and CSA, respectively, while the enhancement for FEDA is 57.3. It is clear that FEDA uses less time than SSA and CSA on the condition that the target signal reaches the same enhancement because SSA and CSA have to iterate a few times. With the number of elements at 4096, in SSA and CSA, the optimization need to be conducted for 16,384 measurements, in which a total of 16,384 pictures were taken, and the intensity integration at the target area was processed. In FEDA, 5460 measurements were conducted, which saves two thirds of the time.

The optimization operations are the processes used to make all of the optimized elements in phase so that the contributions from all of the elements would form constructive interference at the target, therefore, enhancement saturations are reached. However, the experimentally achieved enhancement values are much lower than theoretical values[2]. The main reasons are the environmental noise, instability of the systems, etc. The discrepancy between the experimental and theoretical lies in the standard deviation or the noise level of our system.

The intensity distributions of the transmission light on the image plane after employing the optimized phase distribution on the SLM with 4096 elements are shown in Fig. 4. Figure 4(a) shows the phase distribution of an incident plane wave employed on the SLM, and the corresponding intensity distribution after the plane wave passing through the turbid media is shown in Fig. 4(b). The scattered light forms a random speckle pattern evenly distributed on the whole imaging plane in the statistical

point of view. Figures 4(c), 4(e), and 4(g) show the finally optimized phase distribution on the SLM acquired from the SSA, CSA, and FEDA approaches, respectively, while Figs. 4(d), 4(f), and 4(h) show the achieved corresponding focusing by the wavefront shaping. The optimized phase distributions obtained from the three algorithms are not the same, but they are similar. The correlation coefficients of the optimized phase distributions are 0.87 (for SSA and CSA), 0.85 (for SSA and FEDA), and 0.91 (for CSA and FEDA). It can be seen that in the same experimental environment, the three algorithms reach almost the same focusing result, indicating that the optimized phase distributions are very close to the ideal phase distribution. The enhancement of the target area of Figs. 4(d), 4(f), and 4(h) with respect to Fig. 4(b) are 56.7, 58.5, and 57.3, respectively.

The turbid media is described as the TM elements t_{mn}. This matrix relates the fields of the scattered light to the incident light;

$$E_m = \sum_n^N t_{mn} A_n \exp(\mathrm{i}\phi_n), \qquad (2)$$

where E_m is output light field, and $A_n(x, y)$ and $\phi_n(x, y)$ are the amplitude and phase of the incident light field from element n, respectively. m stands for the number of elements m on the CCD, and N is the number of elements on the SLM. It can be seen from Eq. (2) that the output light field is the result of interference of all of the elements in the incident plane. Equation (2) is the physics principle behind the scattering processing at coherent light illumination, where constructive interference of incident channels after the turbid medium determines the intensity distribution in the output plane. Therefore, modulating the phase distribution level on the SLM at which the light from all elements reach optically in phase at the defined target would be the ultimate goal in optimization processing. Because consideration of the contribution from all elements is taken in every measurement step, no iteration is required in the FEDA approach; therefore, less time is needed compared to the SSA and CSA approaches, in which constructive interference could only be achieved after at least four iterations.

In conclusion, three phase optimization algorithms, SSA, CSA, and the proposed FEDA, are compared in terms of enhancement values and converging rates in forward focusing through a turbid medium. Experiments using the SLM to focus light through ground glass are conducted and compared among the three approaches. From the experimental results, it is concluded that the FEDA has a faster converging rate than those of the CSA and SSA. The reason that FEDA is superior to SSA and CSA is that the contribution from all of the elements is evaluated in every optimization measurement. FEDA can be a feasible idea for focusing light through turbid media and can find uses in the field of dynamic measurements in biological tissue and related applications.
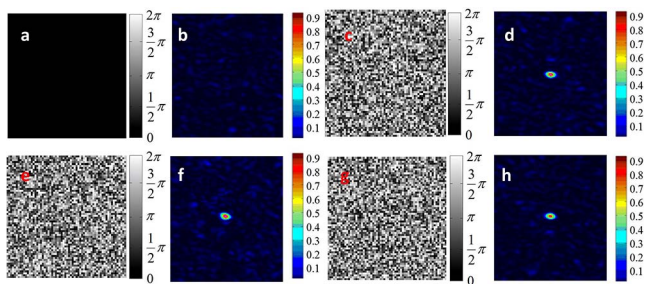

Fig. 4. Optimized phase distribution and transmission images by wavefront shaping. (a) The phase distribution of plane wave, (b) the transmission image through the sample with plane waves, (c) the modulated phase distribution using SSA (after an iteration of four times), (d) the focusing on the CCD using SSA, (e) the modulated phase distribution using CSA (after four iterations), (f) the focusing on the CCD using CSA, (g) the modulated phase distribution using FEDA, and (h) the focusing on the CCD using FEDA.

References

1. I. M. Vellekoop, "Controlling the propagation of light in disordered scattering media," Ph.D. Thesis (University of Twente, 2008).
2. I. M. Vellekoop and A. P. Mosk, Opt. Commun. **281**, 3071 (2007).
3. I. M. Vellekoop and A. P. Mosk, Opt. Lett. **32**, 2309 (2007).
4. I. M. Vellekoop and C. M. Aegerter, Proc. SPIE **7554**, 755430 (2010).
5. I. M. Vellekoop, M. Cui, and C. Yang, Appl. Phys. Lett. **101**, 081108 (2012).
6. T. R. Hillman, T. Yamauchi, W. Choi, R. R. Dasari, M. S. Feld, Y. Park, and Z. Yaqoob, Sci. Rep. **3**, 1909 (2013).
7. D. B. Conkey, A. N. Brown, A. M. Caravacaaguirre, and R. Piestun, Opt. Express **20**, 4840 (2012).
8. D. B. Conkey, A. M. Caravacaaguirre, and R. Piestun, Opt. Express **20**, 1733 (2012).
9. D. Akbulut, T. J. Huisman, E. G. van Putten, W. L. Vos, and A. P. Mosk, Opt. Express **19**, 4017 (2011).
10. I. M. Vellekoop, A. Lagendijk, and A. P. Mosk, Nat. Photon. **4**, 320 (2010).
11. T. Chaigne, O. Katz, A. C. Boccara, M. Fink, E. Bossy, and S. Gigan, Nat. Photon. **8**, 58 (2013).
12. S. M. Popoff, G. Lerosey, R. Carminati, M. Fink, A. C. Boccara, and S. Gigan, Phys. Rev. Lett. **104**, 100601 (2010).
13. S. M. Popoff, G. Lerosey, M. Fink, A. C. Boccara, and S. Gigan, New J. Phys. **13**, 123021 (2011).
14. J. Yoon, K. Lee, J. Park, and Y. Park, Opt. Express **23**, 10158 (2015).
15. M. Kim, W. Choi, Y. Choi, C. Yoon, and W. Choi, Opt. Express **23**, 12648 (2015).
16. S. Tripathi, R. Paxman, T. Bifano, and K. Toussaint, Jr., Opt. Express **20**, 16067 (2012).
17. M. Cui and C. Yang, Opt. Express **18**, 3444 (2010).
18. G. F. Gao, J. Z. Zhao, and Z. X. Fu, Adv. Mater. Res. **1027**, 262 (2014).
19. O. Katz, E. Small, and Y. Silberberg, Nat. Photon. **6**, 549 (2012).
20. H. He, Y. Guan, and J. Zhou, Opt. Express **21**, 12539 (2013).
21. T. Wang, Y. Ding, X. Ji, and D. Zhao, Chin. Opt. Lett. **13**, 102901 (2015).
22. Z. Wu, Q. Shang, T. Qu, Z. Li, and L. Bai, Chin. Opt. Lett. **13**, 121602 (2015).
23. H. Xia, Y. Xiao, H. Li, and S. Tao, Chin. Opt. Lett. **13**, S21201 (2015).